

Real-Time Bioluminescence Imaging of Nitroreductase in Mouse Model

Ping Feng,^{†,‡} Huateng Zhang,^{§,‡} Quankun Deng,[¶] Wei Liu,[¶] Linghui Yang,[¶] Guobo Li,[¶] Guo Chen,[¶] Lupei Du,[§] Bowen Ke,^{*,¶} and Minyong Li^{*,§}

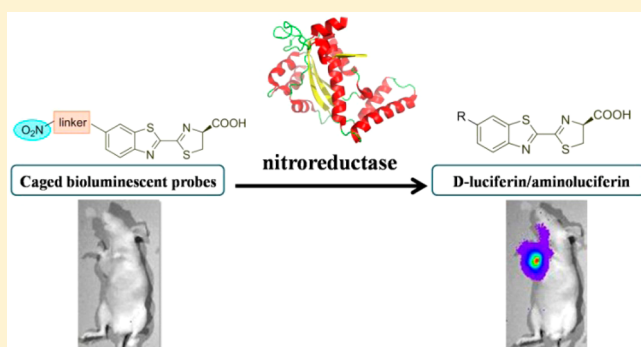
[†]Institute of Clinical Trials, West China Hospital, Sichuan University, Chengdu, Sichuan 610041, China

[¶]The Laboratory of Anesthesiology and Critical Care Medicine, Translational Neuroscience Center, West China Hospital, Sichuan University, Chengdu, Sichuan 610041, China

[§]Department of Medicinal Chemistry, Key Laboratory of Chemical Biology (MOE), School of Pharmacy, Shandong University, Jinan, Shandong 250012, China

Supporting Information

ABSTRACT: Nitroreductase (NTR) is an endogenous reductase overexpressed in hypoxic tumors; however, its precise detection in living cells and animals remains a considerable challenge. Herein, we developed three reaction-based probes and a related bioluminescence assay for the real-time NTR detection. The high sensitivity and selectivity of probe 3, combined with its remarkable potential of bioluminescence imaging, affords a valuable approach for in vivo imaging of NTR in a tumor model mouse.



Hypoxia, defined as a condition of oxygen deprivation in the tissue level to induce cell death if severe or prolonged, occurs during the onset and development of diverse diseases, including cancer, vascular ischemia,^{1,2} and inflammatory disease.³ As a pathophysiological characteristic resulting from poor perfusion and anemia within the malignant solid tumor, low oxygen tension causes a transcription program so as to promote an aggressive tumor phenotype in association with increased metastasis, poor prognosis, and resistance to radiation therapy.⁴ As such, an accurate and reliable hypoxia detection would be beneficial to discern tumor status and identify pathological variables, as well as predict anticancer treatment efficacy. Though direct evidence of hypoxia in human cancers was shown by using oxygen-sensitive electrodes, an invasive nature of electrode measurement may cause inconsistent results in a spatial distribution of hypoxia, because of regional heterogeneity in the tumor.⁵ Accordingly, hypoxia detection strategies have been moving away from direct oxygen measurement to the indirect evaluation of a related biological state or condition, such as bioreductive metabolism and hypoxia-inducible factor.

As a biomarker involved in the transcriptional response to low oxygen tension, nitroreductase (NTR) is directly correlated to the degree of hypoxia in solid tumor.⁶ NTR can catalyze the reduction of nitro groups on aromatic compounds in the presence of a cofactor, such as nicotinamide adenine dinucleotide (NADH) or nicotinamide adenine dinucleotide phosphate (NADPH).⁷ Using this reductive activity, NTR has

been widely employed as an activating enzyme in developing and screening anticancer nitroaromatic prodrug.^{8,9} Given the importance of NTR to diagnosis and treatment of a tumor, so far, great efforts have been undertaken to develop a variety of optical NTR probes, among which specific fluorescent and chemiluminescent NTR probes were fashioned to operate as a valuable toolkit in a biological application.^{10–19} However, the intrinsic photobleaching and autofluorescence of fluorescent probe, as non-negligible flaws of fluorescence modality, restrict its further applications.

It is most desirable that an ideal probe for in vivo imaging should possess indispensable properties, such as high sensitivity, deep tissue penetration, rapid molecular diffusion, and excellent biocompatibility. In order to construct a promising approach for localizing NTR and visualizing its dynamic changes in a living animal, we sought to employ firefly bioluminescence imaging (BLI) as a noninvasive alternative owing to its ability to afford high-sensitivity in vivo imaging.²⁰ Without a detectable light signal from mammalian cells or tissues, bioluminescence imaging during the transformation of D-luciferin into oxyluciferin in the presence of luciferase and other cofactors such as ATP, O₂, and Mg²⁺ features low background and high signal-to-noise contrast, which obviates the intrinsic limitations of fluorescence and provides a sensitive

Received: March 23, 2016

Accepted: May 20, 2016

optical approach to monitoring molecular and cellular events in living animals. By using the luciferase/luciferin system, highly responsive bioluminescent probes have been well established for specific biomolecules of interest, such as caspase,²¹ β -galactosidase,²² β -lactamase,²³ aminopeptidase N,²⁴ hydrogen peroxide,^{24,25} fluoride,²⁶ and hydrogen sulfide.^{27,28} Recently, an NTR bioluminescence sensor (probe 2) was reported with striking features including high selectivity and a robust turn-on for the whole cell and lysate samples.²⁹ In the current study, we presented a highly selective and sensitive bioluminescent probe with improvements for the detection of nitroreductase in living cells and animals.

In designing an NTR bioluminescent reporter, we first envisaged chemoselective probes based on a luciferin/luciferase system as a responsive platform with different caged groups and linkers, which may afford variances on reactivity between probe and analyte. Utilizing the reductive characteristic of the enzyme, turn-on probes with the introduction of nitro group may possess high selectivity and reactivity toward NTR. Upon a selective reduction in which the nitro group was transformed into the amino group and the subsequent cleavage reaction, small molecule probes could be unmasked to release free firefly luciferin for activating the catalytic reaction with luciferase and subsequently producing a photon. To demonstrate our initial hypothesis, bioluminescent probes 1–3 with appropriate NTR-responsive groups were well designed as depicted in Figure 1.

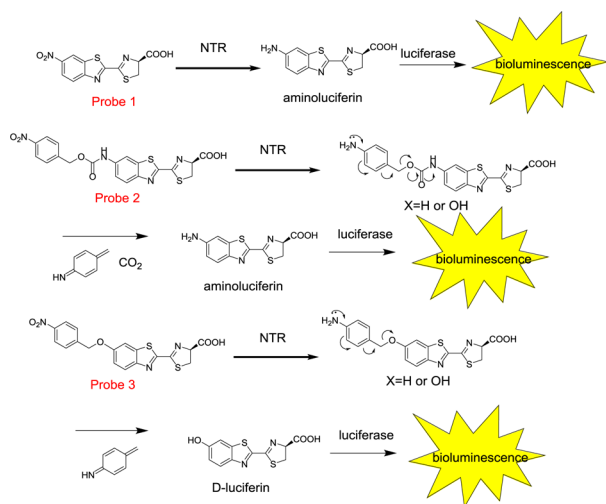


Figure 1. Scheme of bioluminescent probes for selective detection of nitroreductase.

To design and prepare probe 1, aminoluciferin scaffold was substituted with a nitro group, which could be easily reduced to an amino group by nitroreductase. Probe 2 was well designed and synthesized by using a nitro-substituted benzylic linker to acylate the 6'-NH₂ group of aminoluciferin. As an involutive linker, this caging group could be triggered by the reduction of nitro group and release aminoluciferin to produce light. We also designed and prepared bioluminescent probes 3 via introducing a self-immolative linker into luciferin scaffold at the 6'-position. The detailed synthesis and structural characterization are provided in the [Supporting Information](#).

Initial experiments focused on the evaluation of NTR detection efficiency of these probes in an aqueous environment at physiological pH. We first evaluated their responsiveness and related sensitivity of these probes to NTR in a concentration-

dependent manner. Without NTR, all probes were expected to be stable and have a weak bioluminescent response in Tris-HCl buffer in the presence of luciferase and ATP. After being incubated with a series of concentrations of NTR at 37 °C within 60 min, probes were triggered to release free firefly luciferin (or aminoluciferin) and subsequently to provide a robust turn-on response in bioluminescence intensity (Figure S1). Among these molecules, probe 3 exhibited distinctive response capability and high sensitivity to nitroreductase. In response to NTR (5 μ g/mL), probe 3 presented a 552-fold bioluminescent enhancement. Even when the concentration of NTR was as low as 0.001 μ g/mL, a considerable growth (20%) of bioluminescence intensity still can explicitly be observed (Figure S1). Moreover, varying from 0 to 2.5 μ g/mL of NTR, the relative bioluminescence intensity could reflect a real "linear" growth ($R^2 = 0.99$), which could be used to quantify the concentration of NTR. These results fully indicated that probes are capable of interacting with NTR at various concentrations in aqueous systems.

To further assess the selectivity of probes toward NTR in aqueous systems, a range of pertinent species were tested in a bioluminescent assay, including D-cysteine (Cys), sodium ascorbate (VcNa), sodium hydrosulfide (NaSH), β -nicotinamide adenine dinucleotide (NADH), and sodium hyposulfite ($\text{Na}_2\text{S}_2\text{O}_4$). As shown in Figure 2, our bioluminescent probes

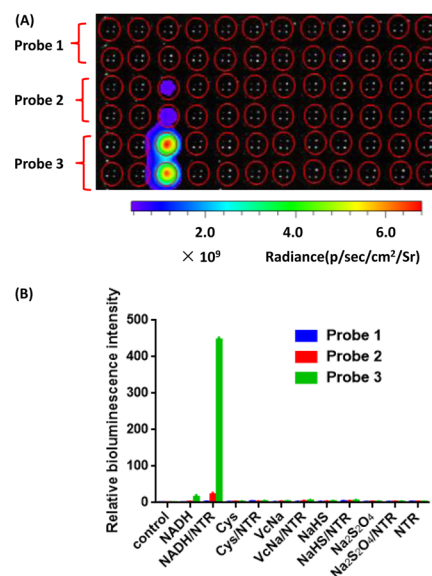


Figure 2. (A) Bioluminescence imaging of selectivity of the probes 1–3 with various relevant reductants (NADH, NTR, Cys, VcNa, NaSH, $\text{Na}_2\text{S}_2\text{O}_4$) after adding luciferase and ATP in a 96-well plate; (B) quantification of the relative bioluminescent intensity of probes for each condition.

(60 μ M) showed no to little bioluminescent response to these reductants, even if their concentrations were high up to 10 mM. However, after adding NADH and NTR simultaneously, the remarkable enhancements to a different extent in bioluminescence intensity were measured (2.24-, 20-, and 450-fold increase for probes 1, 2, and 3, respectively). As a result, probe 3 with high sensitivity and selectivity, combined with favorable characteristics of the bioluminescence technique, can afford potential utility for cellular and in vivo imaging.

Following the preceding characterization of probes, we determined probe 3 as a versatile molecule for further study in

bioimaging, due to its unique features compared to other probes. To test the performance of probe 3 for detecting endogenous NTR in living-cell assays, cobalt chloride was utilized to stimulate luciferase-transfected 4T1 (4T1-luc) cells to elevate the intracellular NTR level.^{19,30} As a result, upon gradual growth of concentrations (0–62.5 μM) of CoCl_2 , sustained increases in bioluminescence intensity were detected before the attainment of the maximum value (186% relative increase) at 62.5 μM CoCl_2 , as shown in Figure 3. It was

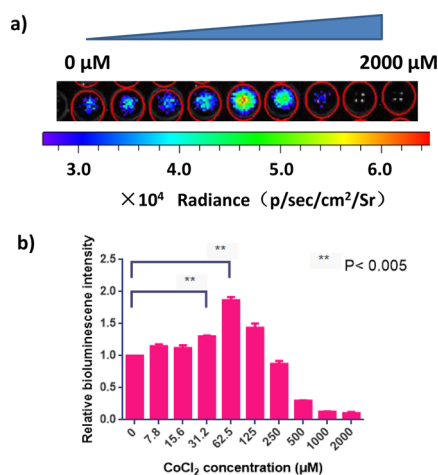


Figure 3. Imaging the endogenous nitroreductase activities in 4T1-luc cells by using probe 3. (a) Bioluminescence imaging of living cells simulated with diverse concentrations (0, 7.8, 15.6, 31.25, 62.5, 125, 250, 500, 1000, 2000 μM) of cobalt chloride; (b) quantification of bioluminescent intensity of probe 3 for each condition.

revealed that not only CoCl_2 can effectively stimulate cell cultures to promote NTR production but also probe 3 is capable of monitoring dynamic changes in NTR level at cellular concentrations. The biocompatibility of all probes was examined by standard MTT assays. It was demonstrated that all probes exhibited very low cytotoxicity to the cultured cells (Figure S2). With rising concentrations of CoCl_2 incubated with living cells, the bioluminescent signal was substantially attenuated in this live-cell assay. Therefore, we proposed that the cell death resulting from the toxicity of CoCl_2 at high concentrations was a reasonable cause (Figure S3).

Having confirmed that probe 3 can offer a highly selective and sensitive approach for monitoring oscillations of endogenous NTR in living cells, we moved on to investigate whether this capability of probe 3 in cell cultures translated to the whole animal. Considering the critical roles of NTR in cancer progression, a breast cancer mouse model was established, in which 1×10^6 4T1-luc cell lines were orthotopically implanted by s.c. injection into nude mice to build 4T1 breast tumor model. After 10 days, a tumor-bearing mouse model with a 1.6 cm diameter was formed. In the present study, dicoumarol as a reductase inhibitor was utilized to decrease NTR activity in the control group.^{8,19} Different groups were injected with probe 3 into the tumor, and time-dependent signal changes were collected every 5 min within 70 min as shown in Figure 4. Due to the enzymatic inhibition, there is little to no bioluminescence growth observed in the control group, in which hypoxia tumor was pretreated with dicoumarol. In contrast, a progressive increase in bioluminescence intensity was immediately detected within the first few minutes after probe injection, and the highest

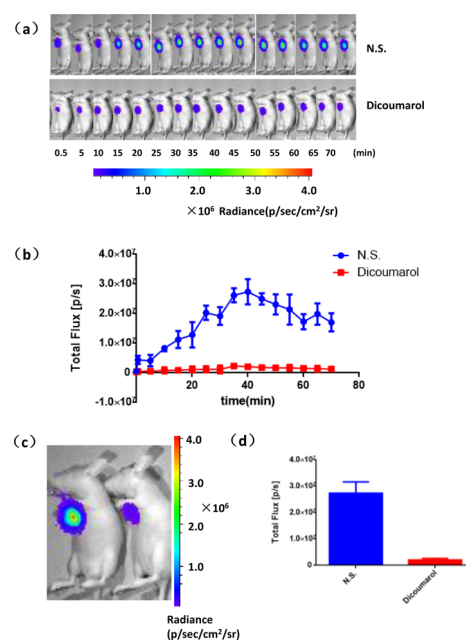


Figure 4. Bioluminescence imaging of endogenous nitroreductase activities in 4T1 tumor mouse model by using probe 3. (a) Time-dependent bioluminescence imaging of mouse tumor model with or without injection of dicoumarol; (b) quantification of the total flux of (a); (c) representative bioluminescence imaging at 40 min with (right) or without (left) injection of dicoumarol; (d) quantification of the total flux of (c).

bioluminescence was reached in 40 min with ca. a 10-fold increasing signal in the tumor region relative to the control animal. These results in the enzyme inhibition experiment not only confirmed the long-term responsiveness of probe 3 toward endogenous NTR in living animal but also verified that the performance of probe 3 was carried out through the reductive mechanism of NTR.

In an effort to expand the mission of probe 3 to visualize the degree of hypoxia in the process of tumor growth in living animal, we assessed the possibility of bioluminescent tracking of fluctuations in endogenous NTR level in the tumor model by using this unique chemical tool. For this purpose, different sized A549 tumors (1.0 and 1.3 cm) in living mice were respectively injected with probe 3 and the subsequent change of bioluminescence intensity was kinetically recorded. As shown in Figure 5, the distinct enhancements in emission signal from the tumor regions were observed within the first few minutes after injection of probe 3. The increased bioluminescence intensity from whole tumors measurably lasted for more than 30 min, and the maximum values were reached within 5.5 min after injection. The average flux value of the 1.3 cm-diameter tumor was 5-fold higher than that of the 1.0 cm-diameter tumor at 5.5 min. These results clearly not only established a clear correlation between dynamic NTR degrees and different sized tumors but also suggested that probe 3 is capable of providing a valuable tool for monitoring alterations of endogenous NTR in tumor development.

In brief, herein we developed a bioluminescent probe for the chemoselective visualization of endogenous NTR in hypoxia tumor model. Even in complex biological systems, probe 3 exhibited high selectivity, sensitivity, and other favorable properties, which presents a powerful tool in bioimaging and provides a viable approach for visualizing NTR overexpression

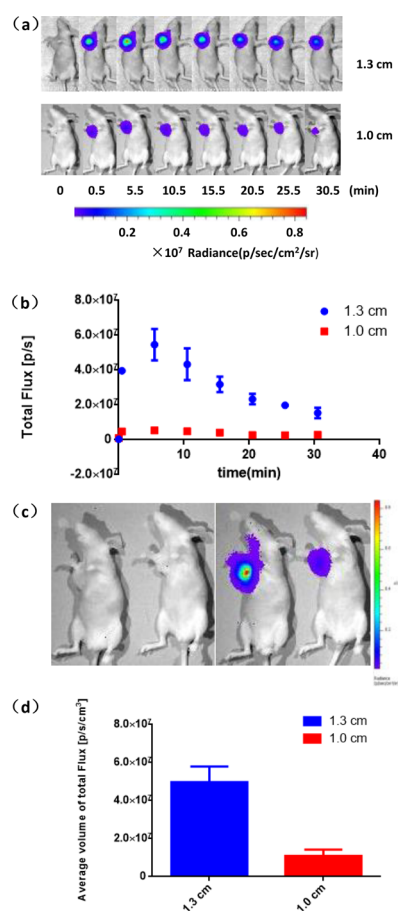


Figure 5. Bioluminescence imaging of endogenous nitroreductase overexpressed in A549 tumor mouse model by using probe 3: (a) time-dependent bioluminescence imaging of different sized tumors (1.3 and 1.0 cm); (b) total flux changing from tumor region at 0–30 min; (c) bioluminescence imaging of different sized tumors at 5.5 min; (d) the average volume of the total flux from different sized tumor regions at 5.5 min.

and related hypoxia degree in the tumor. By using this bioimaging technique, we offer a valuable opportunity to understand NTR/hypoxia degree and their roles in tumor processes.

■ ASSOCIATED CONTENT

● Supporting Information

The Supporting Information is available free of charge on the ACS Publications website at DOI: 10.1021/acs.analchem.6b01160.

Full experimental procedure, NMR, MS, fluorescence, and cell imaging data. (PDF)

■ AUTHOR INFORMATION

Corresponding Authors

*Tel./Fax: +86-28-8518-8632. E-mail: bowenke80@hotmail.com (B.K.).

*Tel./Fax: +86-531-8838-2076. E-mail: mli@sdu.edu.cn (M.L.).

Author Contributions

‡P.F. and H.Z. contributed equally.

Notes

The authors declare no competing financial interest.

■ ACKNOWLEDGMENTS

We are grateful for financial support from the National Natural Science Foundation of China (Nos. 21402130 and 81273471), the National Program on Key Basic Research Project (No. 2013CB734000), the Program for Changjiang Scholars and Innovative Research Team in University (No. IRT13028), the Major Project of Science and Technology of Shandong Province (No. 2015ZDJS04001), the Shandong Key Research & Development Project (No. 2015GSF118166), and the Fundamental Research Funds of Shandong University (No. 2014JC008).

■ REFERENCES

- (1) Semenza, G. L. *Annu. Rev. Med.* **2003**, *54*, 17–28.
- (2) Crawford, J. H.; Isbell, T. S.; Huang, Z.; Shiva, S.; Chacko, B. K.; Schechter, A. N.; Darley-Usmar, V. M.; Kerby, J. D.; Lang, J. D.; Kraus, D. *Blood* **2006**, *107*, 566–574.
- (3) Murdoch, C.; Muthana, M.; Lewis, C. E. *J. Immunol.* **2005**, *175*, 6257–6263.
- (4) Harris, A. L. *Nat. Rev. Cancer* **2002**, *2*, 38–47.
- (5) Walsh, J. C.; Lebedev, A.; Aten, E.; Madsen, K.; Marciano, L.; Kolb, H. C. *Antioxid. Redox Signaling* **2014**, *21*, 1516–1554.
- (6) Wilson, W. R.; Hay, M. P. *Nat. Rev. Cancer* **2011**, *11*, 393–410.
- (7) Bryant, D.; McCalla, D.; Leeksa, M.; Laneville, P. *Can. J. Microbiol.* **1981**, *27*, 81–86.
- (8) Johansson, E.; Parkinson, G. N.; Denny, W. A.; Neidle, S. J. *Med. Chem.* **2003**, *46*, 4009–4020.
- (9) Atwell, G. J.; Yang, S.; Pruijn, F. B.; Pullen, S. M.; Hogg, A.; Patterson, A. V.; Wilson, W. R.; Denny, W. A. *J. Med. Chem.* **2007**, *50*, 1197–1212.
- (10) Shi, Y.; Zhang, S.; Zhang, X. *Analyst* **2013**, *138*, 1952–1955.
- (11) Guo, T.; Cui, L.; Shen, J.; Zhu, W.; Xu, Y.; Qian, X. *Chem. Commun.* **2013**, *49*, 10820–10822.
- (12) Cui, L.; Zhong, Y.; Zhu, W.; Xu, Y.; Du, Q.; Wang, X.; Qian, X.; Xiao, Y. *Org. Lett.* **2011**, *13*, 928–931.
- (13) Yuan, J.; Xu, Y.-Q.; Zhou, N.-N.; Wang, R.; Qian, X.-H.; Xu, Y.-F. *RSC Adv.* **2014**, *4*, 56207–56210.
- (14) Li, Z.; Li, X.; Gao, X.; Zhang, Y.; Shi, W.; Ma, H. *Anal. Chem.* **2013**, *85*, 3926–3932.
- (15) Xu, J.; Sun, S.; Li, Q.; Yue, Y.; Li, Y.; Shao, S. *Analyst* **2015**, *140*, 574–581.
- (16) Xu, K.; Wang, F.; Pan, X.; Liu, R.; Ma, J.; Kong, F.; Tang, B. *Chem. Commun.* **2013**, *49*, 2554–2556.
- (17) Bae, J.; McNamara, L. E.; Nael, M. A.; Mahdi, F.; Doerksen, R. J.; Bidwell, G. L.; Hammer, N. I.; Jo, S. *Chem. Commun.* **2015**, *51*, 12787–12790.
- (18) Cao, J.; Campbell, J.; Liu, L.; Mason, R. P.; Lippert, A. R. *Anal. Chem.* **2016**, *88*, 4995.
- (19) Li, Y.; Sun, Y.; Li, J.; Su, Q.; Yuan, W.; Dai, Y.; Han, C.; Wang, Q.; Feng, W.; Li, F. *J. Am. Chem. Soc.* **2015**, *137*, 6407–6416.
- (20) Li, J.; Chen, L.; Du, L.; Li, M. *Chem. Soc. Rev.* **2013**, *42*, 662–676.
- (21) Thornberry, N. A.; Rano, T. A.; Peterson, E. P.; Rasper, D. M.; Timkey, T.; Garcia-Calvo, M.; Houtzager, V. M.; Nordstrom, P. A.; Roy, S.; Vaillancourt, J. P.; Chapman, K. T.; Nicholson, D. W. *J. Biol. Chem.* **1997**, *272*, 17907–17911.
- (22) GEIGER, R.; SCHNEIDER, E.; WALLENFELS, K.; MISKA, W. *Biol. Chem. Hoppe-Seyler* **1992**, *373*, 1187–1192.
- (23) Yao, H.; So, M.-k.; Rao, J. *Angew. Chem., Int. Ed.* **2007**, *46*, 7031–7034.
- (24) Wu, W.; Li, J.; Chen, L.; Ma, Z.; Zhang, W.; Liu, Z.; Cheng, Y.; Du, L.; Li, M. *Anal. Chem.* **2014**, *86*, 9800–9806.
- (25) Van de Bittner, G. C.; Dubikovskaya, E. A.; Bertozzi, C. R.; Chang, C. J. *Proc. Natl. Acad. Sci. U. S. A.* **2010**, *107*, 21316–21321.
- (26) Ke, B.; Wu, W.; Wei, L.; Wu, F.; Chen, G.; He, G.; Li, M. *Anal. Chem.* **2015**, *87*, 9110–9113.

- (27) Ke, B.; Wu, W.; Liu, W.; Liang, H.; Gong, D.; Hu, X.; Li, M. *Anal. Chem.* **2016**, *88*, 592–595.
- (28) Tian, X.; Li, Z.; Lau, C.; Lu, J. *Anal. Chem.* **2015**, *87*, 11325–11331.
- (29) Wong, R. H.; Kwong, T.; Yau, K.-H.; Au-Yeung, H. Y. *Chem. Commun.* **2015**, *51*, 4440–4442.
- (30) Jiang, J.; Auchinvole, C.; Fisher, K.; Campbell, C. J. *Nanoscale* **2014**, *6*, 12104–12110.